Molecular Vision 2017; 23:740-752 <http://www.molvis.org/molvis/v23/740>
Received 23 May 2017 | Accepted 12 October 2017 | Published 14 October 2017

Elucidating the molecular basis of PPCD: Effects of decreased ZEB1 expression on corneal endothelial cell function

Marina Zakharevich, Jaffer M. Kattan, Judy L. Chen, Benjamin R. Lin, Aleck E. Cervantes, Doug D. Chung, Ricardo F. Frausto, Anthony J. Aldave

(The first two authors contributed equally to this work.)

Stein Eye Institute, David Geffen School of Medicine at UCLA, Los Angeles, CA

Purpose: To investigate the functional role that the *zinc e-box binding homeobox 1* (*ZEB1*) gene, which underlies the genetic basis of posterior polymorphous corneal dystrophy 3 (PPCD3), plays in corneal endothelial cell proliferation, apoptosis, migration, and barrier function.

Methods: A human corneal endothelial cell line (HCEnC-21T) was transfected with siRNA targeting *ZEB1* mRNA. Cell proliferation, apoptosis, migration, and barrier assays were performed: Cell proliferation was assessed with cell counting using a hemocytometer; cell apoptosis, induced by either ultraviolet C (UVC) radiation or doxorubicin treatment, was quantified by measuring cleaved caspase 3 (cCASP3) protein levels; and cell migration and barrier function were monitored with electric cell–substrate impedance sensing (ECIS).

Results: *ZEB1* knockdown in HCEnC-21T cells transfected with siRNA targeting *ZEB1* did not result in a significant difference in cell proliferation when compared with control. Although knockdown of *ZEB1* in HCEnC-21T cells sensitized the cells to UV-induced apoptosis, *ZEB1* knockdown did not alter the cells' susceptibility to doxorubicin-induced apoptosis, as measured with cCASP3 protein levels, compared with controls. Similarly, no difference was observed in cell migration following *ZEB1* knockdown. However, cell barrier function increased significantly following *ZEB1* knockdown.

Conclusions: The corneal endothelium in PPCD3 is characterized by morphologic, anatomic, and molecular features that are more consistent with an epithelial-like rather than an endothelial-like phenotype. Although these characteristics have been well documented, we demonstrate for the first time that susceptibility to UV-induced apoptosis and cell barrier function are significantly altered in the setting of reduced *ZEB1*. The significance of an altered cellular response to apoptotic stimuli and increased cell barrier function in the pathobiology of PPCD remains to be fully elucidated.

Posterior polymorphous corneal dystrophy (PPCD) is a genetically heterogeneous, autosomal dominant disease that alters corneal endothelium morphology with a concomitant reduction in visual acuity. Clinical symptoms vary from asymptomatic to significant stromal edema requiring corneal transplantation in about 20–25% of cases [1,2]. PPCD has been mapped to two genetic loci, the first on chromosome 20 (PPCD1) and the second on chromosome 10 (PPCD3), in which mutations in the *ovo-like 2* (*OVOL2*; Gene ID: 58495; OMIM: 616441) and *zinc e-box binding homeobox 1* (*ZEB1;* Gene ID: 6935; OMIM: 189909) genes have been identified, respectively [2-7]. Nonsense, frameshift, and copy number mutations in *ZEB1* associated with PPCD are predicted to reduce the amount of available wild-type *ZEB1* and lead to *ZEB1* haploinsufficiency, which is the underlying presumed cause of PPCD3 [8-17]. *OVOL2*, which is not expressed in the corneal endothelium, encodes a transcription factor that suppresses the transcription of *ZEB1* [18,19]. Thus, in PPCD1, it is predicted that the identified c.-307T>C mutation in the *OVOL2* promoter leads to ectopic expression of OVOL2 in the corneal endothelium and subsequent repression of *ZEB1* transcription, effectively resulting in *ZEB1* haploinsufficiency.

The human corneal endothelium expresses several markers associated with the mesenchymal phenotype (e.g., *CDH2* [Gene ID: 1000; OMIM: 114020], *VIM* [Gene ID: 7431; OMIM: 193060], and *ZEB1*) and lacks the expression of markers associated with the epithelial phenotype (e.g., *CDH1* [Gene ID: 999; OMIM: 192090] and *OVOL2*). ZEB1 and OVOL2 are transcription factors that have demonstrated an inverse relationship in corneal epithelial cells and cancer cell lines with respect to cell states along the bidirectional epithelial to mesenchymal transition (EMT) spectrum, with increasing levels of ZEB1 tipping the balance toward the mesenchymal state, and increasing OVOL2 levels tipping the balance toward the epithelial cell state [20,21]. ZEB1 and OVOL2 constitute a mutually inhibitory circuit for mediating bidirectional EMT, a process important in

Correspondence to: Anthony J. Aldave, The Jules Stein Eye Institute, 100 Stein Plaza, UCLA, Los Angeles, CA 90095-7003; Phone: (310) 206-7202; FAX: (310) 794-7906; email: aldave@jsei.ucla.edu

embryogenesis, tissue maintenance, and promoting stem cell properties [21,22]. In addition, ZEB1 and OVOL2 have been shown to coordinate the pathologic progression of EMT and mesenchymal to epithelial transition (MET) in cancer [21,23]. Similarly, OVOL2 maintains the corneal epithelial phenotype by coordinated repression of ZEB1 expression and subsequent expression of CDH1 and repression of CDH2 [20]. These patterns of MET-associated gene expression are similar to those observed in PPCD: increased *CDH1* and decreased *CDH2* expression with concomitant decreased *ZEB1* expression compared with age-matched controls [24]. In PPCD, corneal endothelial cell (CEnC) metaplasia is characterized by the appearance of epithelial-like features, such as stratification of the normal endothelial monolayer, the expression of epithelial cell-associated keratins, and downregulation of endothelial-specific genes [24-26]. Reduced ZEB1 expression in PPCD results from *ZEB1* haploinsufficiency due to either ZEB1 truncation (PPCD3) or ectopic OVOL2 expression (PPCD1). *ZEB1* haploinsufficiency is possibly involved in genetically unresolved cases of PPCD as well, with a reduction in ZEB1 levels sufficient to cause PPCD irrespective of the underlying genetic context.

We hypothesize that PPCD is a disease characterized by dysregulation in ZEB1-dependent gene expression, which is predicted to alter CEnC function and response to mediators of key cellular processes (e.g., cell proliferation, migration, apoptosis, and cell barrier function). While documenting the changes that occur at the transcriptome level in PPCD was the focus of a separate study, we describe the effects of decreased ZEB1 levels on CEnC function, providing insight into the role of ZEB1 in CEnC function and the dysfunction that characterizes PPCD [24].

METHODS

Corneal endothelial cell culture: Cell culture–grade plastic flasks were coated with 40 µg/cm^2 chondroitin sulfate A (Sigma-Aldrich, St. Louis, MO) and 40 ng/cm^2 laminin (L4544; Sigma-Aldrich) in Dulbecco's PBS (1X; 138 mM NaCl, 2.67 mM KCl, 8 mM Na_2HPO_4-$7H_2O$, 1.5 mM KH_2PO_4, pH 7.2) for 2 h. Telomerase-immortalized human corneal endothelial cells (HCEnC-21T) were grown in a 1:1 mixture of F12-Ham's medium and M199 medium (Life Technologies, Grand Island, NY), supplemented with 5% (v/v) fetal bovine serum (Atlanta Biologicals, Flowery Branch, GA), 20 µg/ml human recombinant insulin (Life Technologies), 20 µg/ml ascorbic acid (Sigma Aldrich), 10 ng/ml recombinant human fibroblast growth factor (FGF)-basic (Peprotech, Rocky Hill, NJ), 100 µg/ml penicillin (Life Technologies), and 100 µg/ml streptomycin (Life Technologies) [27]. The cell line was maintained in a humidified chamber containing 5% CO_2. The HCEnC-21T cell line was generated from a cadaveric donor cornea, and the establishment and characterization of this cell line were described in 2012 [27]. In that report, the authors demonstrated that the cell line retains human corneal endothelial cell function and the expression of corneal endothelial–associated genes. In addition, we recently performed transcriptomic analysis of the HCEnC-21T cell line (obtained directly from the laboratory that generated the line) and demonstrated that the HCEnC-21T cell line expresses genes specific to the human corneal endothelium (i.e., no expression in the human corneal epithelium and keratocytes) to a greater extent than two other corneal endothelial cell lines [28]. Moreover, the HCEnC-21T cell line was established by retroviral transduction of the human telomerase reverse transcriptase *(TERT*; Gene ID: 7015; OMIM: 187270) gene, which is highly expressed in this cell line but absent in ex vivo and primary HCEnC [28].

STR analysis for the authentication of the HCEnC-21T cells: Genomic DNA was isolated from HCEnC21T cells using the FlexiGene DNA Kit (Qiagen, Valencia, CA) and submitted to Laragen Sequencing and Genotyping (Laragen, Culver City, CA) for short tandem repeat (STR) analysis. Authentication was performed using the PowerPlex® 16 System (Promega, Madison, WI), a multiplex STR system that allows for the analysis of 16 loci and complies with ANSI/ATCC ASN-0002–2011 guidelines for cell line authentication. The STR profile obtained for the HCEnC-21T cells was compared with the STR profiles available in the German Collection of Microorganisms and Cell Cultures database (DSMZ GmbH, Braunschweig, Lower Saxony, Germany; Appendix 1 and Appendix 2). As STR analysis was not performed for the HCEnC-21T cells by the originating laboratory (personal communication), a comparison with the DSMZ STR profile database did not identify a perfect match. However, the HCEnC-21T STR profile demonstrated similarity (78% match) to the STR profile for a human mammary gland/breast epithelium (184B5; American Type Culture Collection, Manassas, VA) but did not reach the threshold (>80%) for relatedness.

Selection of and corneal endothelial cell transfection with ZEB1 siRNAs: An initial test of three *ZEB1* siRNAs was performed to determine the ability of each siRNA to knock down ZEB1 protein levels. HCEnC-21T cells were transfected with 10 nM of *ZEB1* siRNA (siRNA-A: rArCrArArGrArUrArCrUrArGrCrUrCrArGrArArGrGrArGTA, siRNA-B: rArCrArArUrArCrArArGrArGrGrUrUrArArArGrGrArArGCT or siRNA-C: rGrGrCrCrUrArCrArArUrArArCrUrArGrCrArUrUrUrGrUTG; OriGene Technologies, Rockville, MD).

All transfections were performed using Lipofectamine® LTX (Life Technologies) according to the manufacturer's recommendations. A scrambled siRNA (OriGene Technologies) was used as a control. Detection of ZEB1 with western blotting demonstrated that *ZEB1* siRNA-A and siRNA-C produced the most robust reduction of the ZEB1 protein (Appendix 3), and thus, they were used in subsequent experiments.

Determination of ZEB1 knockdown with western blotting: Before each functional assay was performed, the efficacy of *ZEB1* siRNA-mediated knockdown of the ZEB1 protein in the HCEnC-21T cells was confirmed with western blotting. In brief, whole-cell protein lysates were prepared by lysing HCEnC-21T cells with radioimmunoprecipitation assay (RIPA) buffer. Ten micrograms of total protein were resolved with sodium dodecyl sulfate–polyacrylamide gel electrophoresis (SDS–PAGE) and transferred on a 0.45 µm polyvinylidene difluoride (PVDF) membrane. ZEB1 was detected using an anti-ZEB1 antibody (3396; Cell Signaling, Beverly, MA), and detection of alpha tubulin (TUBA) using an anti-TUBA antibody (3873; Cell Signaling) was used as a loading control. Secondary antibodies conjugated to horseradish peroxidase (HRP) were used for substrate (Luminata™ Forte HRP substrate; Millipore) conversion to the chemiluminescence signal (Table 1). Chemiluminescence was visualized with the exposure of Hyperfilm (GE Healthcare Bio-Sciences, Marlborough, MA). Densitometric analysis for alpha tubulin (50 kDa) and ZEB1 (125 kDa) protein levels was performed using ImageJ software [29].

Corneal endothelial cell proliferation assay: HCEnC-21T cells were reseeded at 10% confluence 24 h after transfection. The number of cells (N) was counted using a hemacytometer. Cell numbers were obtained at 3 (defined as N_0), 24, 48, and 72 h (N_t) after seeding. Cell numbers were normalized and graphed as the ratio N_t/N_0.

Corneal endothelial cell apoptosis assays: HCEnC-21T cells were reseeded 24 h after transfection. At 48 h post-transfection, the cells were irradiated with 50 mJ/m^2 of UVC radiation using a Stratagene Stratalinker 1800. Whole-cell protein lysates were prepared at 0, 2, 4, 6, and 8 h after UVC radiation treatment. Apoptosis was also induced by treating cells with 2.5 µM doxorubicin hydrochloride (Sigma-Aldrich) for 0, 6, 10, 14, and 18 h. Whole-cell protein lysates were prepared at each time point.

Assessment of apoptosis induction with detection of caspase 3 cleavage: Apoptosis was measured with western blotting for the appearance of cleaved caspase 3 (cCASP3) products, which are generated upon proteolytic activation of zymogenic caspase 3 [30]. Whole-cell protein lysates were prepared by lysing HCEnC-21T cells with RIPA buffer. Ten micrograms of total protein were resolved with SDS–PAGE and transferred onto a 0.45 µm PVDF membrane. cCASP3 proteins were detected using anti-cCASP3 (9661; Cell Signaling), and TUBA, used as a loading control, was detected using an anti-TUBA antibody (3873; Cell Signaling; Table 1). Secondary antibodies conjugated to HRP were used for substrate conversion to the chemiluminescence signal (Luminata™ Forte HRP substrate; Millipore; Table 1). Chemiluminescence was visualized with the exposure of Hyperfilm (GE Healthcare Bio-Sciences, Marlborough, MA). Densitometric analysis for alpha tubulin (50 kDa) and cCASP3 (14 kDa (non-specific), 17 kDa (active), and 19 kDa) protein levels was performed using ImageJ software.

Corneal endothelial cell wound healing (migration) assay: 8W1E electric cell–substrate impedance sensing (ECIS) Cultureware™ disposable electrode arrays (Applied BioPhysics, Troy, NY) were stabilized with F99 medium according to the manufacturer's protocol and then were coated with 40 µg/cm^2 chondroitin sulfate A (Sigma-Aldrich) and 400 ng/cm^2 laminin (Sigma-Aldrich) in PBS for 2 h. Twenty-four hours after transfection, the HCEnC-21T cells were reseeded at 100% confluency in the stabilized electrode arrays. The arrays were incubated at 37 °C for an additional 24 h, allowing cells to attach to the electrodes. At 24 h after reseeding, a circular gap in the cell layer above each electrode

Table 1. Antibodies used for western blot.

Target protein	Isotype	Immunogen species	Clonality	Dilution	Vendor	Catalog number
Primary antibodies						
ZEB1	rabbit IgG	human	mono	1:500	Cell Signaling Technology	3396
cCASP3	rabbit IgG	human	poly	1:100	Cell Signaling Technology	9661
TUBA	mouse IgG	human	mono	1:4000	Cell Signaling Technology	3873
Secondary antibodies						
Rb-IgG	goat IgG	rabbit	poly	1:40000	Millipore	AP132P
Ms-IgG	goat IgG	mouse	poly	1:40000	Millipore	AP124P

was generated by applying the cell wounding module to the electrode array at a current of 1400 µA, a frequency of 60,000 Hz, and a duration of 20 s. Cell migration across the gap was monitored by measuring the resistance (ohms) at the electrode using an ECIS Zθ and 16W array station with ECIS software (Applied BioPhysics).

Corneal endothelial cell barrier assay: 8W10E+ ECIS Cultureware™ disposable electrode arrays (Applied BioPhysics) were stabilized with F99 medium according to the manufacturer's protocol. The arrays were subsequently coated with 40 µg/cm^2 chondroitin sulfate A (Sigma-Aldrich) and 400 ng/cm^2 laminin (Sigma-Aldrich) in PBS for 2 h. Forty-eight hours after transfection, HCEnC-21T cells were reseeded at 100% confluency in the coated and stabilized electrode arrays. The arrays were incubated at room temperature for 1 h, allowing the cells to attach to the electrodes. Measured in ohms, cell resistances at multiple frequencies were monitored using an ECIS Zθ and 16W array station with ECIS software (Applied BioPhysics). To describe three properties (cell attachment to a growth surface, cell–cell contact, and plasma membrane composition) of cells in a monolayer, modeling of the impedance spectra obtained with ECIS was performed using the ECIS software, which utilizes previously described fundamental electrophysiology principles [31]. The modeling results in the ability to describe the constraint of current flow within the subcellular space (i.e., resistance to current flow as a consequence of cell attachment to a growth surface; alpha), constraint of current flow within the intercellular space (i.e., resistance to current flow as a consequence of the density of cell–cell contacts; Rb), and the capacitance of the cell membrane (i.e., capacitance as a result of the composition and morphology of the plasma membrane; Cm).

Statistical analyses: All statistical analyses performed and graphs generated using GraphPad Prism software (GraphPad Software, La Jolla, CA). Unless otherwise noted, all results are representative of a minimum of three replicates.

RESULTS

Reduced ZEB1 expression does not alter corneal endothelial cell proliferation: ZEB1 protein levels were markedly reduced in the HCEnC-21T cells by transfection with either of two different siRNAs targeting *ZEB1* (siRNA-A or siRNA-C). ZEB1 protein levels were measured with western blotting at 48 h post-transfection, when the cells were reseeded for the cell proliferation assay (Figure 1A). Cell proliferation was measured and calculated as a ratio of cell number at time N_t (where t = 24, 48, or 72 h) divided by the cell number at N_0 (Figure 1B). The ZEB1 reduction in the HCEnC-21T cells did not result in a statistically significant difference in cell proliferation at 24, 48, or 72 h compared with scrambled siRNA control (sc-siRNA).

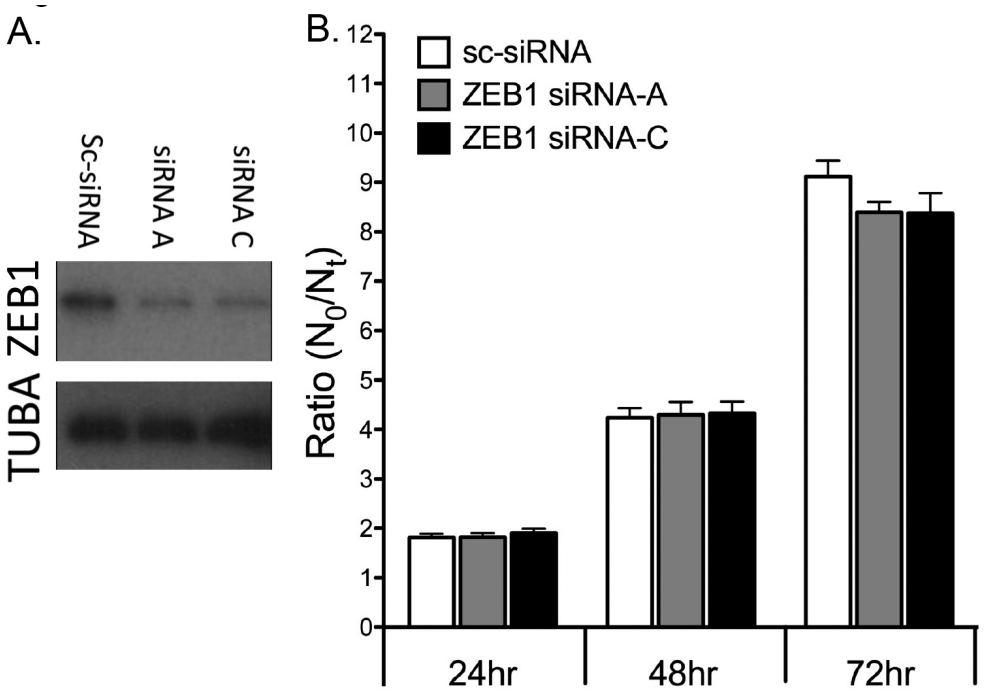

Figure 1. Cell proliferation in HCEnC-21T cells transfected with siRNA. Cells were transfected with scrambled siRNA (sc-siRNA), *ZEB1* siRNA-A, or *ZEB1* siRNA-C. **A**: ZEB1 knockdown was demonstrated by western blotting for ZEB1, with TUBA used as a loading control. **B**: Cell quantities at 24, 48, and 72 h (N_t) were compared to the initial quantity (N_0), and plotted as the ratio N_t/N_0. Results represent 12 independent data points (n=12). Error bars = standard error of the mean (SEM).

Reduced ZEB1 expression increases corneal endothelial cell susceptibility to UV-induced, but not doxorubicin-induced, apoptosis:

UVC-induced apoptosis—The ZEB1 protein levels were markedly reduced in the HCEnC-21T cells transfected with either *ZEB1* siRNA-A or *ZEB1* siRNA-C compared to the sc-siRNA transfected cells at 48 h post-transfection (i.e., 0 h UVC) and at each 2 h time point following UVC irradiation (Figure 2A–C). Although siRNA-A produced greater knockdown of ZEB1 in the HCEnC-21T cells compared with *ZEB1* siRNA-C, siRNA-C (and not siRNA-A) made the cells more susceptible to UV-induced apoptosis. The active 17 kDa cCASP3 (and the non-specific 14 kDa) protein levels were statistically significantly increased 6 and 8 h after UVC irradiation with siRNA-C compared with siRNA-A and sc-siRNA (Figure 2D,E). However, no statistically significant difference was noted in the 19 kDa cCASP3 protein levels at any time point after transfection with siRNA-A or -C (Figure 2F).

Doxorubicin-induced apoptosis—The HCEnC-21T cells transfected with either siRNA-A or siRNA-C were observed to have markedly lower ZEB1 protein levels compared to the sc-siRNA transfected cells at 48 h post-transfection (i.e., 0 h doxorubicin [DOX]) and at each 2 h time point following DOX treatment (Figure 3A–C). Although the 17 and 19 kDa cCASP3 (and the non-specific 14 kDa) protein levels were higher in the siRNA-A transfected cells than in the sc-siRNA transfected cells at the 10, 14, and 18 h time points following DOX exposure, the difference was not statistically significant at any of the time points (Figure 3D–F). Similarly, the differences between the 17 and 19 kDa cCASP3 (and the non-specific 14 kDa) protein levels in the siRNA-C transfected cells and the sc-siRNA transfected cells were not statistically significantly different at any time point (Figure 3D–F).

Reduced ZEB1 expression does not alter corneal endothelial cell migration: The effect of reduced ZEB1 protein levels on corneal endothelial cell migration was assessed with ECIS. Transfection of HCEnC-21T cells with siRNA-C resulted in markedly reduced ZEB1 protein levels compared to cells transfected with sc-siRNA (Figure 4A). Forty-eight hours following transfection and 24 h after seeding at 100% confluence on an ECIS electrode array, a high current was applied to clear a central circular area. Thereafter, migration of the cells into the cleared zone was measured for up to 12 h (24–36

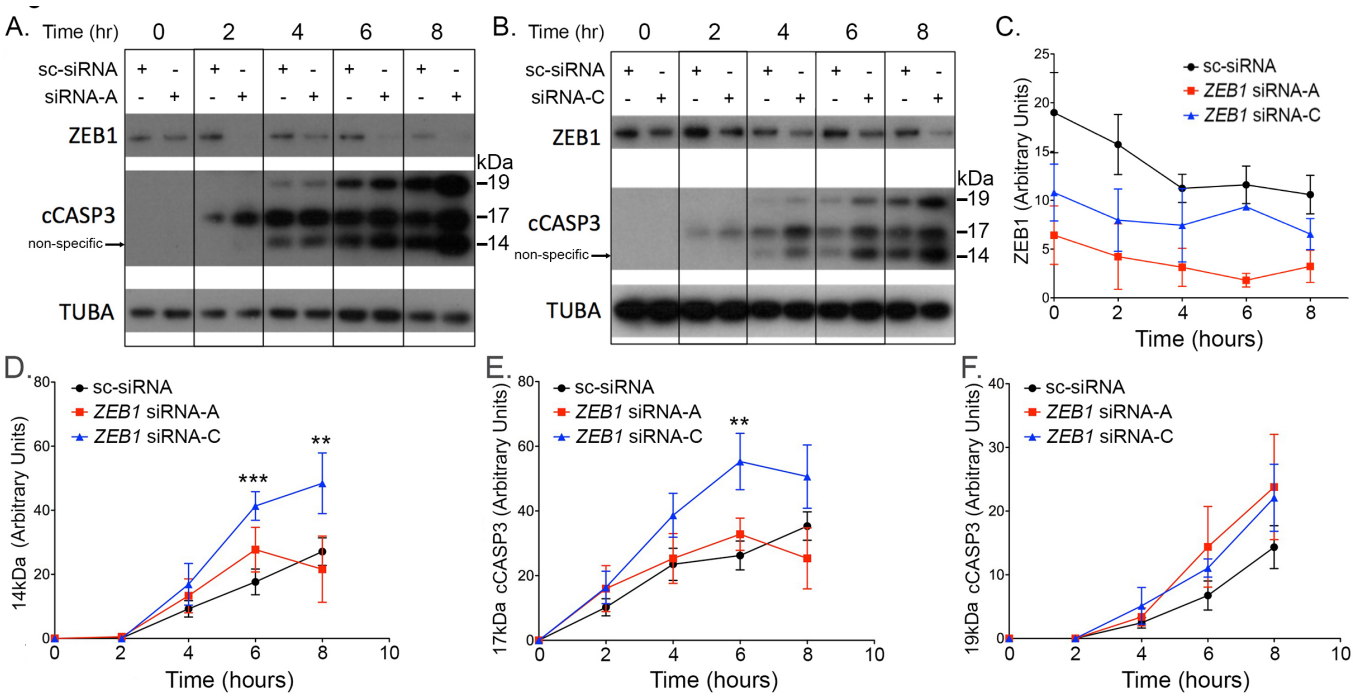

Figure 2. Quantification of UV-induced apoptosis in ZEB1 knockdown cells. **A**, **B**: HCEnC-21T cells were transfected with *ZEB1* siRNA-A, *ZEB1* siRNA-C, or scrambled siRNA (sc-siRNA) and exposed to ultraviolet (UV) light for 0, 2, 4, 6, and 8 h. Apoptosis was assessed by the appearance of cleaved caspase 3 (cCASP3) with western blotting. **C**: ZEB1 knockdown was assessed with western blotting, quantified, and graphed. Abundance of the 14 kDa (**D**; non-specific), 17 kDa (**E**; active), and 19 kDa (F) fragments of cCASP3 was quantified with western blotting and graphed. Results represent three independent experiments (n = 3). Error bars = standard error of the mean (SEM), and **p<0.01 and ***p<0.001.

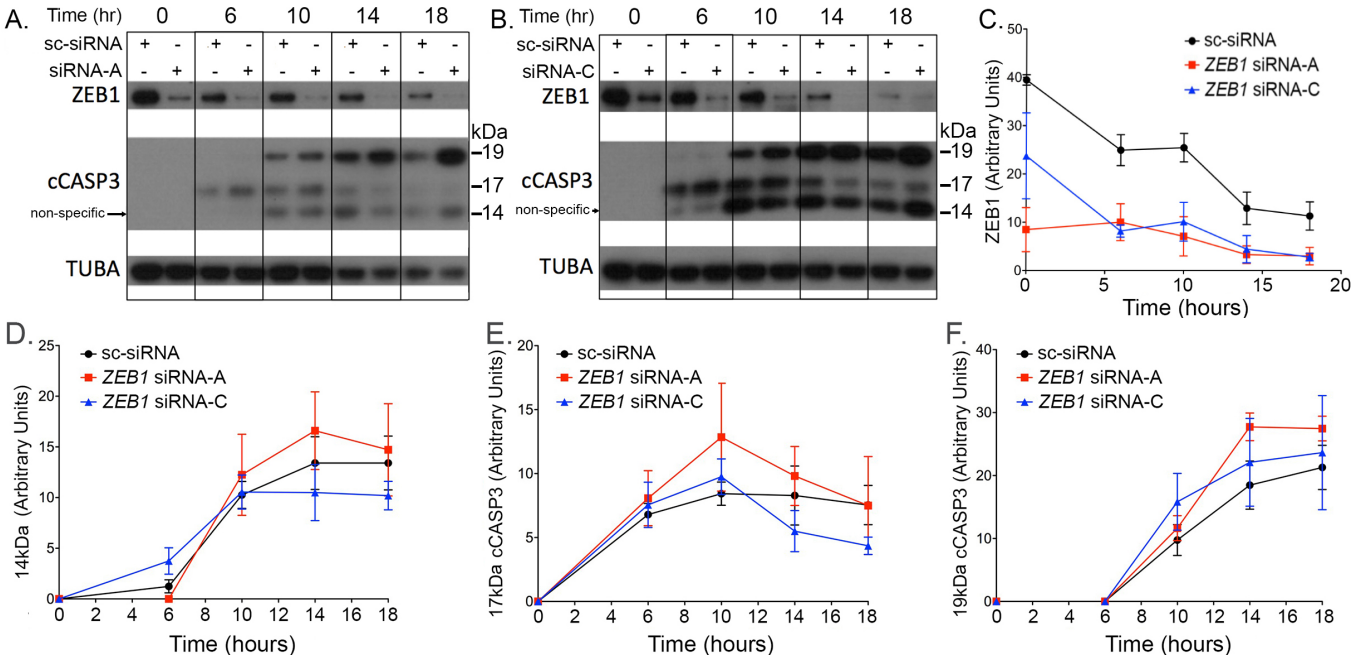

Figure 3. Quantification of DOX-induced apoptosis in ZEB1 knockdown cells. **A**, **B**: HCEnC-21T cells were transfected with *ZEB1* siRNA-A, *ZEB1* siRNA-C, or scrambled siRNA (sc-siRNA), and exposed to DOX for 0, 6, 10, 14, and 18 h. Apoptosis was assessed by the appearance of cleaved caspase 3 (cCASP3) with western blotting. **C**: ZEB1 knockdown was assessed with western blotting, quantified, and graphed. Abundance of the 14 kDa (**D**; non-specific), 17 kDa (**E**; active), and 19 kDa (**F**) fragments of cCASP3 was quantified with western blotting and graphed. Results represent three independent experiments (n = 3). Error bars = standard error of the mean (SEM).

h range). No statistically significant difference was observed in the cell migration rate in the HCEnC-21T cells transfected with *ZEB1* siRNA-C compared with the sc-siRNA transfected cells (Figure 4B).

Reduced ZEB1 expression increases corneal endothelial cell barrier function: The impact of reduced ZEB1 expression on corneal endothelial cell barrier function was assessed with ECIS. The HCEnC-21T cells were transfected with either *ZEB1* siRNA-C or sc-siRNA, with markedly reduced ZEB1 protein levels in the *ZEB1* siRNA transfected cells (Figure 5A). Forty-eight hours post-transfection, cells were seeded at 100% confluence on an electric impedance array, and electrical resistance was measured for 48 h. Impedance (ohms) measured for the *ZEB1* siRNA transfected cells was statistically significantly higher from 30 to 48 h compared with the control cells ($p<0.05$; Figure 5B). Modeling of the impedance spectra demonstrated a statistically significant increase in cell attachment resistance (alpha) observed at early (9–20 h) and late (38–46 h) phases for the *ZEB1* siRNA-C transfected cells compared with the control cells ($p<0.05$; Figure 5C). In addition, a statistically significant increase in inter-endothelial cell resistance (Rb) was observed between 7 and 48 h for the *ZEB1* siRNA-C transfected cells compared with the control cells ($p<0.05$; Figure 5D). No statistically significant difference was observed in the plasma membrane capacitance (Cm; Figure 5E).

DISCUSSION

Posterior polymorphous corneal dystrophy was first reported in 1916, with the description of the appearance of "bullous" lesions on the posterior surface of the cornea [32]. Other clinical features associated with PPCD (e.g., iridocorneal adhesions, glaucoma, and keratoconus) were described over the next several decades [1,33-37]. Histopathologic, electron microscopic, and immunologic studies revealed that the corneal endothelium in PPCD is characterized by epithelial-like characteristics, including a multilaminar organization, desmosomal junctions, dense microvilli, sparse mitochondria, and the expression of keratin proteins [1,26,37-39]. In a recent study of the corneal endothelial transcriptome in PPCD, we identified ectopic or increased expression of many corneal epithelial-associated genes (e.g., *KRT12* [Gene ID: 3859; OMIM: 601687], *DSG3* [Gene ID: 1830; OMIM: 169615], and *CDH1*), decreased expression of many endothelial-associated genes (e.g., *VIM* and *CDH2*), and decreased expression of many corneal endothelial-specific genes (e.g., *ETNPPL* [Gene ID: 64850; OMIM: 614682], *PIP5K1B* [Gene ID: 8395; OMIM: 602745], and *LRRN1*) identified in a previous study

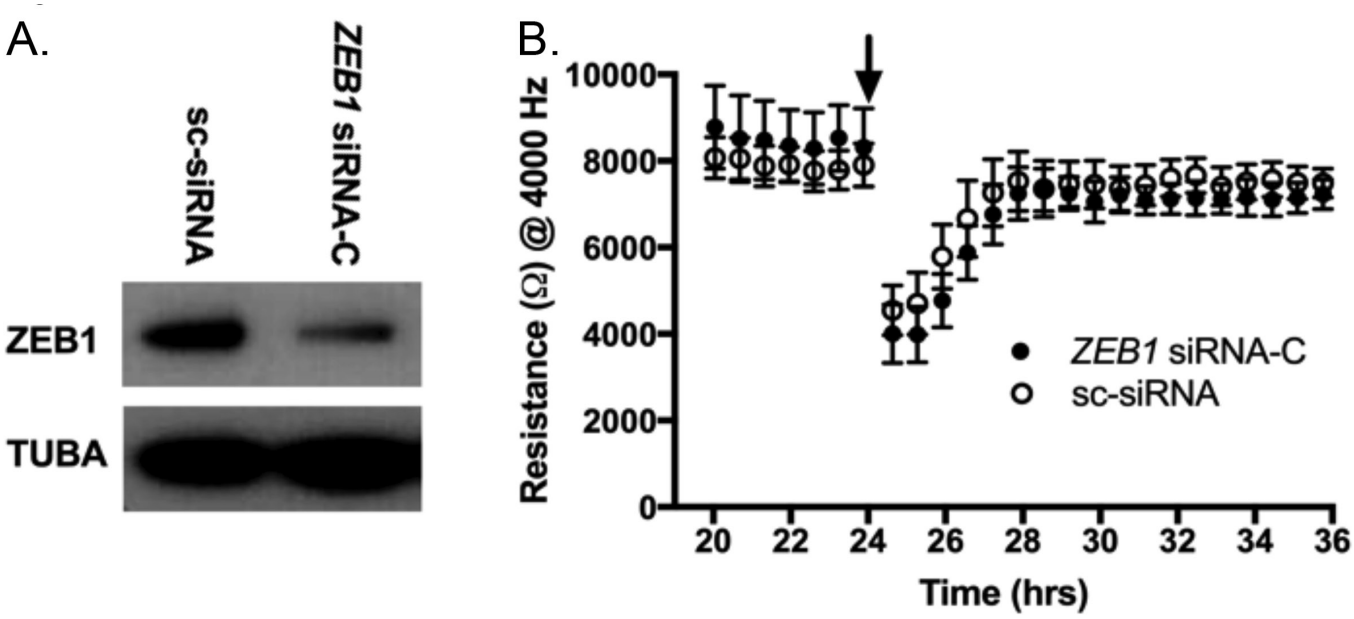

Figure 4. The impact of ZEB1 reduction on cell migration in HCEnC-21T cells. **A**: HCEnC-21T cells were transfected with either *ZEB1* siRNA-C or scrambled siRNA (sc-siRNA), and knockdown of ZEB1 was validated with western blotting. **B**: Transfected HCEnC-21T cells were seeded to 100% confluence on an electric cell–substrate impedance sensing (ECIS) electrode array. A high current (arrow) was applied to the circular electrode underneath the central region of the cell monolayer, thus clearing the circular area. Migration of cells into the cleared area was monitored for 12 h after wounding by measuring impedance (ohms) across the electrode at 4,000 Hz. Three wells for each condition were measured; n = 3. Error bars = standard error of the mean (SEM).

[24,28]. In addition, endothelial cells dissociated from PPCD corneas and grown in culture demonstrated the same features observed in ex vivo tissue, with the added observation that the PPCD endothelial cells possess a higher capacity for proliferation [40]. Recently, studies using in vivo confocal microscopy have observed polymorphic endothelial cells with hyperreflective nuclei in PPCD-affected individuals [41,42]. Taken together, these findings support the conclusion that the corneal endothelium in PPCD demonstrates an epithelial phenotype.

Although the evidence to support the assertion that PPCD endothelium possesses an epithelial-like phenotype is compelling, the process by which the cells gain their epithelial nature has yet to be elucidated. However, cell state transition (CST) is an integral process during embryogenesis and generation/maintenance of all human tissues, with misdirection of this process implicated in many pathologic contexts (e.g., congenital malformations, fibrosis, and cancer) [43-45]. CST gives rise to distinct cell states and may provide the most plausible explanation for the apparent epithelialization of the corneal endothelium in PPCD. CST can be generally classified as either a process of EMT or the reverse, MET. EMT is characterized by a "cadherin switch" in which an epithelial cell undergoing EMT "switches" from expressing CDH1 (epithelial (E)-cadherin) to expressing CDH2 (neural (N)-cadherin), and the reverse in the case of MET [46,47]. Distinct epithelial and mesenchymal gene expression profiles have been described with vimentin (VIM), a type III intermediate filament protein, often coexpressed with CDH2 in mesenchymal cells [22]. The fact that ZEB1 and OVOL2 are key players in CST and that mutations in the genes that encode these transcription factors cause PPCD and presumably lead to the appearance of an epithelial cell-like phenotype of the corneal endothelium suggests that CST, or MET in particular, is involved in the development of PPCD [20,21,23,48,49]. Although CEnCs are not true mesenchyme, they express markers associated with the mesenchymal cell state (e.g., ZEB1, VIM, and CDH2) and the degree to which CEnCs resemble true mesenchyme may be dependent on the level of expression of proteins promoting the mesenchymal phenotype, namely, ZEB1. Genetic evidence supports *ZEB1* haploinsufficiency as the cause of PPCD, which suggests that in order for ZEB1 to maintain the CEnC phenotype, ZEB1 must be expressed above a certain threshold [17]. Thus, the absence or the reduction of endogenous ZEB1 levels below this threshold in CEnC presumably leads to an epithelial phenotype [50]. In contrast, increased levels of ZEB1 are associated with the transition of cultured primary CEnC to a fibroblastic phenotype. The transition of primary CEnC to

a fibroblastic (i.e., mesenchymal) cell state in culture may be caused by enzymatic/mechanical dissociation of cell–cell contacts and cell–substrate adhesions and activation of Wnt signaling [51]. This transition is associated with increased expression of the mesenchymal proteins ZEB1, CDH2, and VIM and a concomitant decrease in the tight junction protein TJP1 (or ZO1) compared with ex vivo CEnC [28]. Taken together, these observations implicate ZEB1, a master regulator of cell state transitions, as playing a significant role in CEnC CST.

Endothelial to mesenchymal transition (EnMT) in the human cornea and transforming growth factor beta 1 (TGFβ1)-induced EMT in a mouse cell line demonstrated increased cell proliferation and migration and decreased susceptibility to apoptosis associated with the mesenchymal cell state compared with the endothelial and epithelial cell states [52,53]. Thus, a mesenchymal to endothelial transition (MEnT) or MET may be predicted to elicit the reverse response in these cell processes. Consistent with this, ZEB1 knockdown has been reported to lead to a decrease in cell proliferation and increased susceptibility to apoptosis in human and mouse cell lines, with ZEB1 overexpression eliciting the opposite result [48,54]. However, an increase in corneal endothelial cell proliferation has previously been reported in late-gestation stage *Zeb1* null mice, along with increased expression of cytokeratin, CDH1, and COL4A3 [50]. In addition, increased proliferation of the endothelium has also been described as a clinical manifestation of PPCD. The effect of altered ZEB1 expression in a given cell type depends on whether ZEB1 functions to activate or repress transcription of the target genes in that particular cell type. This, in turn, depends on several factors, including the recruitment of cofactors (corepressors and coactivators) and the presence of canonical Wnt signaling (TCF7L2/beta-catenin), which changes ZEB1 from a repressor to an activator of transcription [55-57]. Thus, although we hypothesized that reduced levels of ZEB1 would lead to an alteration of CEnC proliferation, apoptosis, migration, and barrier function, it was difficult to predict what the effect would be in CEnCs. We found that reduced ZEB1 protein expression in CEnCs did not alter either cell proliferation or cell migration, suggesting that other factors may be involved in regulating

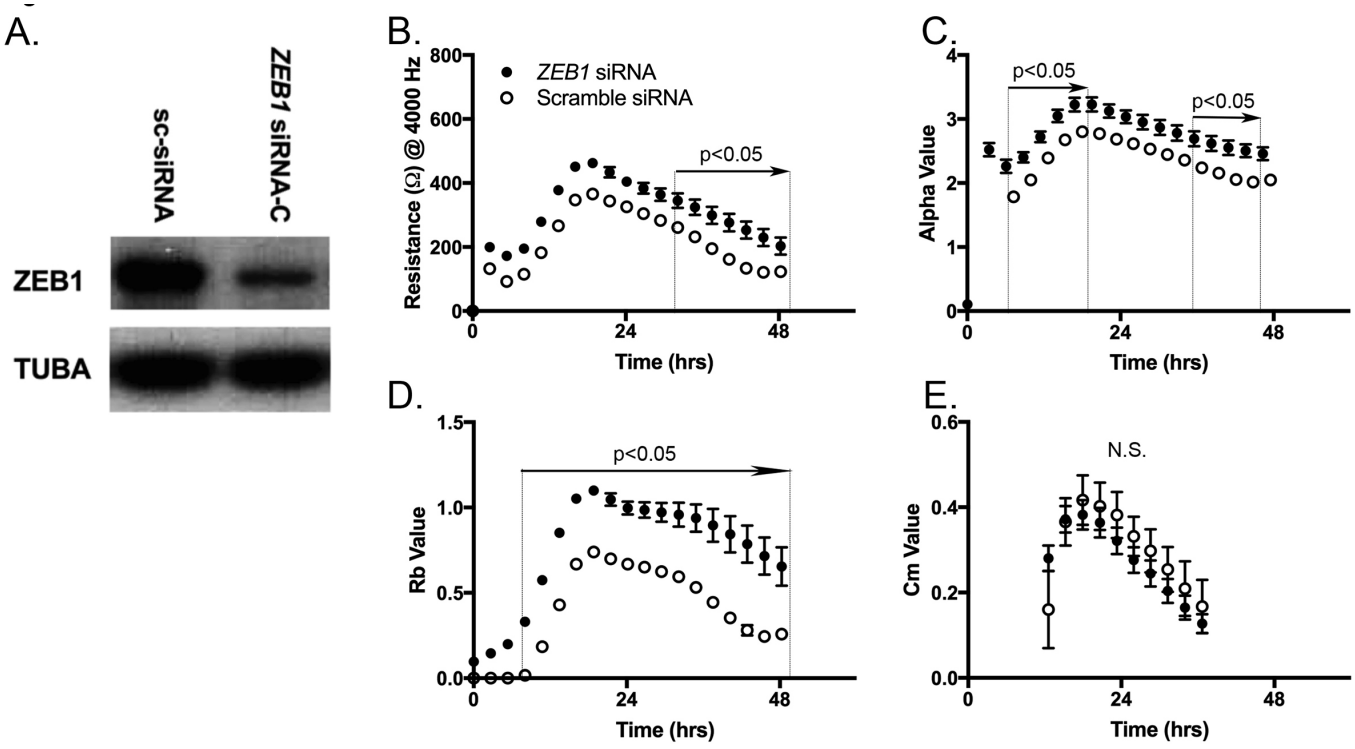

Figure 5. The impact of ZEB1 reduction on cell barrier function in in HCEnC-21T cells. **A**: HCEnC-21T cells were transfected with *ZEB1* siRNA-C or scrambled siRNA (sc-siRNA), and knockdown of ZEB1 was confirmed with western blotting. **B**: Impedance (ohm) at 4,000 Hz, interendothelial resistance (Rb), cell attachment resistance (alpha), and plasma membrane capacitance (Cm) were measured for 48 h after seeding on electric cell–substrate impedance sensing (ECIS) electrode arrays. Three wells for each condition were measured; n = 3. Error bars = standard error of the mean (SEM). Statistical significance ($p<0.05$) is noted for a range when two or more sequential time points demonstrated statistical significance.

the proliferative and migratory capacity of endothelial cells in PPCD.

The observation that ZEB1 knockdown in CEnCs leads to an increased susceptibility to UVC-induced apoptosis (i.e., increased levels of the active 17 kDa fragment of cleaved CASP3) is consistent with previous studies in other cell types that have demonstrated ZEB1 acts as a suppressor of apoptosis and that a reduction of ZEB1 sensitizes cells to apoptotic stimuli [48,54,58]. However, this effect is dependent on the type of apoptotic stimuli because although UVC and DOX induce apoptosis via DNA damage, a lack of impact on cCASP3 levels after DOX treatment suggests that DOX-induced cleavage of caspase 3 occurs in a ZEB1-independent manner. Nevertheless, although apoptosis has not been described as playing a role in the pathogenesis of PPCD, apoptosis may be associated with the observed variable reduction in CEnC density [15,38,59].

The most important functional property of the corneal endothelium is to maintain corneal deturgescence, a relatively dehydrated state of the corneal stroma that is essential to the maintenance of corneal clarity [60,61]. Disruption of the CEnC barrier and/or its pump function leads to corneal edema, which characterizes advanced cases of PPCD. In the present study, we observed that reduced ZEB1 results in an increase in CEnC barrier function, due to increased substrate attachment and intercellular adhesion. Compared with the corneal endothelium, which is functionally classified as a "leaky membrane," corneal epithelial cells demonstrate greater resistance to fluid flow due to significantly higher expression of tight-junction proteins, which regulate intercellular barrier function [28,62,63]. Thus, the observation that *CLDN1* [Gene ID: 9076; OMIM: 603718] and *F11R/JAM1* [Gene ID: 50848; OMIM: 605721], epithelial-associated tight junction genes, are increased in the PPCD endothelium

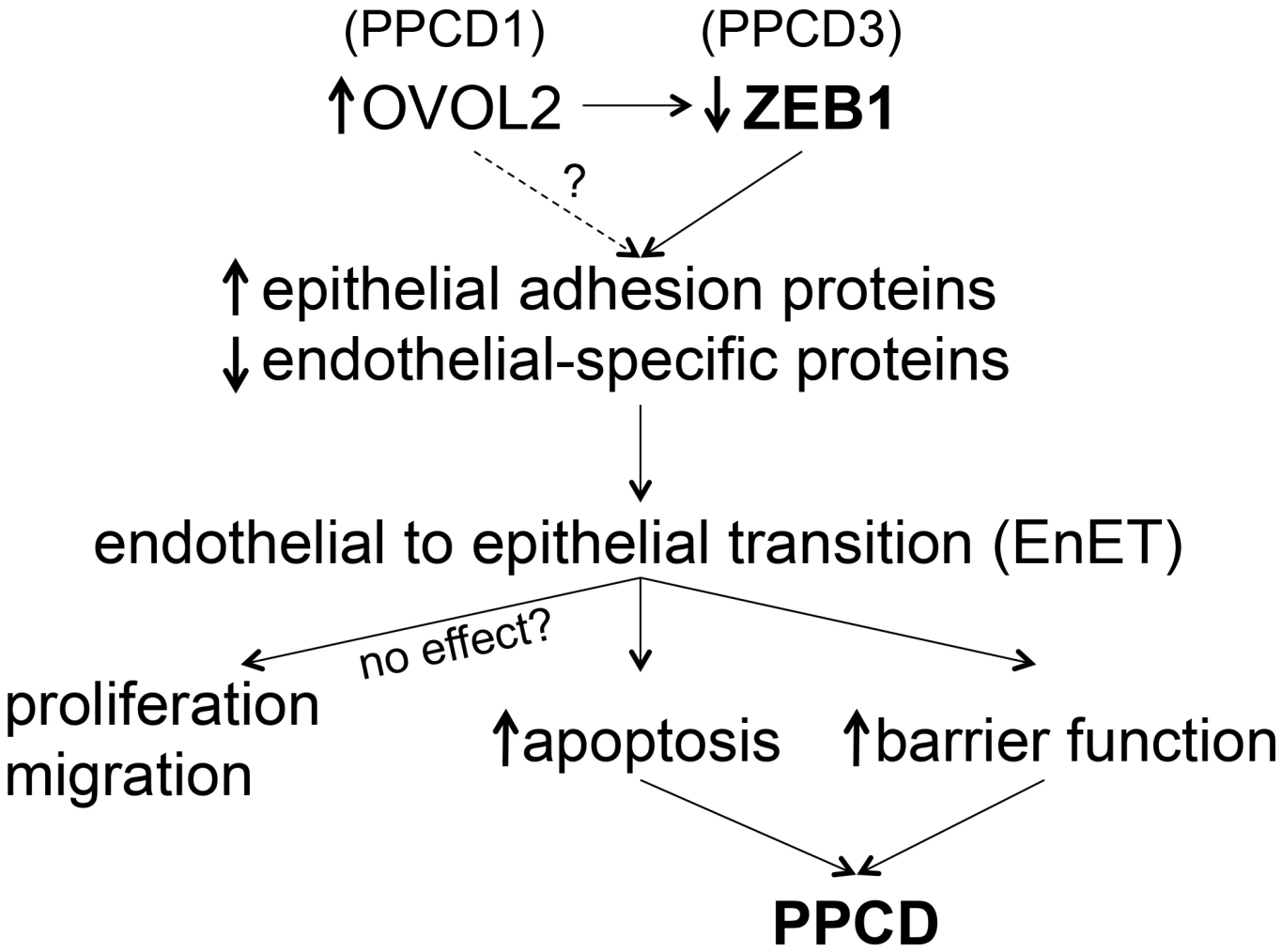

Figure 6. Hypothetical model of the mechanism underlying the progression of genotype to phenotype in posterior polymorphous corneal dystrophy.

may explain the increased resistance observed in our PPCD cell model [24]. In addition, desmosomes, which are typically epithelial-specific complexes that form dense cell–cell contacts, are present in the skin, normal corneal epithelium, and PPCD endothelium but not in the normal endothelium [1,37,38,64,65]. Because paracellular fluid flow is integral to corneal endothelial cell pump function, changes in the integrity and complexity of the endothelial intercellular clefts will alter the dynamics of water flow [66,67]. Dysregulation of CEnC pump function may also be caused by the altered expression of solute transporters, which are important in establishing the gradients that regulate water flow across the endothelium [24,66,67]. In PPCD, CEnC pump function may also be disrupted by the tendency for the endothelium to adopt a multilaminar organization, which may result in an additional physical barrier to fluid flow. As CEnC permeability is presumably decreased in PPCD, endothelial decompensation leading to the need for keratoplasty in approximately one-quarter of affected individuals is most likely due to impairment of the CEnC pump function.

In this study, we report that ZEB1 knockdown in CEnCs leads to increased apoptosis and barrier function, which may explain some of the characteristic features of PPCD. Although we did not observe differences in cell proliferation and migration, their role in PPCD remains an open question because our cell-based system did not consider potential roles in embryogenesis, specifically in differentiation of endothelial precursors. In addition, the in vivo microenvironment may possess factors that modulate CEnC properties for which we could not account in our cell-based system. Nevertheless, we speculate that the observed differences are a consequence of CST, specifically, endothelial to epithelial transition (EnET), which we propose as a subtype of MET (Figure 6). However, we acknowledge that further investigation is needed to determine the full significance of the present results to the pathobiology of PPCD.

APPENDIX 1.

To access the data, click or select the words "Appendix 1." Note: Bold numbers are inconsistent alleles between the HCEnC-21T cells and the best match cell line. BM, best match. *Breast epithelia have the cell line ID number 184B5.

APPENDIX 2.

To access the data, click or select the words "Appendix 2." Electropherograms of analyzed STR alleles using the PowerPlex® 16 System. STRs are indicated in gray boxes above each electropherogram. Numbers under STR peaks refer to allele sizes in repeat units. Single numbers (single peak) indicate a homozygous STR locus, and two numbers (double peaks) indicate a heterozygous STR locus. The gender (female) of the donor was defined by the single peak amplicon at approximately 106 bp resulting from amplification of the X- and Y-specific amelogenin locus. The absence of more than two alleles at each locus suggests that the cell line consists of a pure population of homogenous cells.

APPENDIX 3.

To access the data, click or select the words "Appendix 3." Selection of *ZEB1* siRNA molecules was performed by assessing the efficacy of each to knock down ZEB1 protein expression in corneal endothelial cells. HCEnC-21T cells were transfected with *ZEB1* siRNA-A, -B and -C, and a scrambled siRNA (sc) was used as a control. Cells were lysed at 24, 48 and 72 h post siRNA transfection and ZEB1 levels were assessed by western blotting. *ZEB1* siRNAs A and C demonstrated robust knock down of ZEB1 expression at 48 and 72 h and thus were used for functional assays. TUBA was used as a protein loading control.

ACKNOWLEDGMENTS

Support provided by National Eye Institute Grants 1R01EY022082 (A.J.A.), P30EY000331 (core grant), the Walton Li Chair in Cornea and Uveitis (A.J.A.), the Stotter Revocable Trust and an unrestricted grant from Research to Prevent Blindness.

REFERENCES

1. Krachmer JH. Posterior polymorphous corneal dystrophy: a disease characterized by epithelial-like endothelial cells which influence management and prognosis. Trans Am Ophthalmol Soc 1985; 83:413-75. [PMID: 3914130].

2. Weiss JS, Moller HU, Aldave AJ, Seitz B, Bredrup C, Kivela T, Munier FL, Rapuano CJ, Nischal KK, Kim EK, Sutphin J, Busin M, Labbe A, Kenyon KR, Kinoshita S, Lisch W. IC3D classification of corneal dystrophies–edition 2. Cornea 2015; 34:117-59. [PMID: 25564336].

3. Liskova P, Gwilliam R, Filipec M, Jirsova K, Reinstein Merjava S, Deloukas P, Webb TR, Bhattacharya SS, Ebenezer ND, Morris AG, Hardcastle AJ. High prevalence of posterior polymorphous corneal dystrophy in the Czech Republic; linkage disequilibrium mapping and dating an ancestral mutation. PLoS One 2012; 7:e45495-[PMID: 23049806].

4. Aldave AJ, Han J, Frausto RF. Genetics of the corneal endothelial dystrophies: an evidence-based review. Clin Genet 2013; 84:109-19. [PMID: 23662738].

5. Davidson AE, Liskova P, Evans CJ, Dudakova L, Noskova L, Pontikos N, Hartmannova H, Hodanova K, Stranecky V, Kozmik Z, Levis HJ, Idigo N, Sasai N, Maher GJ,

Bellingham J, Veli N, Ebenezer ND, Cheetham ME, Daniels JT, Thaung CM, Jirsova K, Plagnol V, Filipec M, Kmoch S, Tuft SJ, Hardcastle AJ. Autosomal-Dominant Corneal Endothelial Dystrophies CHED1 and PPCD1 Are Allelic Disorders Caused by Non-coding Mutations in the Promoter of OVOL2. Am J Hum Genet 2016; 98:75-89. [PMID: 26749309].

6. Le DJ, Chung DW, Frausto RF, Kim MJ, Aldave AJ. Identification of Potentially Pathogenic Variants in the Posterior Polymorphous Corneal Dystrophy 1 Locus. PLoS One 2016; 11:e0158467-[PMID: 27355326].

7. Chung DD, Frausto RF, Cervantes AE, Gee KM, Zakharevich M, Hanser EM, Stone EM, Heon E, Aldave AJ. Confirmation of the OVOL2 Promoter Mutation c.-307T>C in Posterior Polymorphous Corneal Dystrophy 1. PLoS One 2017; 12:e0169215-[PMID: 28046031].

8. Krafchak CM, Pawar H, Moroi SE, Sugar A, Lichter PR, Mackey DA, Mian S, Nairus T, Elner V, Schteingart MT, Downs CA, Kijek TG, Johnson JM, Trager EH, Rozsa FW, Mandal MN, Epstein MP, Vollrath D, Ayyagari R, Boehnke M, Richards JE. Mutations in TCF8 cause posterior polymorphous corneal dystrophy and ectopic expression of COL4A3 by corneal endothelial cells. Am J Hum Genet 2005; 77:694-708. [PMID: 16252232].

9. Liskova P, Tuft SJ, Gwilliam R, Ebenezer ND, Jirsova K, Prescott Q, Martincova R, Pretorius M, Sinclair N, Boase DL, Jeffrey MJ, Deloukas P, Hardcastle AJ, Filipec M, Bhattacharya SS. Novel mutations in the ZEB1 gene identified in Czech and British patients with posterior polymorphous corneal dystrophy. Hum Mutat 2007; 28:638-[PMID: 17437275].

10. Aldave AJ, Yellore VS, Yu F, Bourla N, Sonmez B, Salem AK, Rayner SA, Sampat KM, Krafchak CM, Richards JE. Posterior polymorphous corneal dystrophy is associated with TCF8 gene mutations and abdominal hernia. Am J Med Genet A 2007; 143A:2549-56. [PMID: 17935237].

11. Vincent AL, Niederer RL, Richards A, Karolyi B, Patel DV, McGhee CN. Phenotypic characterisation and ZEB1 mutational analysis in posterior polymorphous corneal dystrophy in a New Zealand population. Mol Vis 2009; 15:2544-53. [PMID: 19997581].

12. Nguyen DQ, Hosseini M, Billingsley G, Heon E, Churchill AJ. Clinical phenotype of posterior polymorphous corneal dystrophy in a family with a novel ZEB1 mutation. Acta Ophthalmol 2010; 88:695-9. [PMID: 19432861].

13. Bakhtiari P, Frausto RF, Roldan AN, Wang C, Yu F, Aldave AJ. Exclusion of pathogenic promoter region variants and identification of novel nonsense mutations in the zinc finger E-box binding homeobox 1 gene in posterior polymorphous corneal dystrophy. Mol Vis 2013; 19:575-80. [PMID: 23559851].

14. Lechner J, Dash DP, Muszynska D, Hosseini M, Segev F, George S, Frazer DG, Moore JE, Kaye SB, Young T, Simpson DA, Churchill AJ, Heon E, Willoughby CE. Mutational spectrum of the ZEB1 gene in corneal dystrophies supports a genotype-phenotype correlation. Invest Ophthalmol Vis Sci 2013; 54:3215-23. [PMID: 23599324].

15. Liskova P, Palos M, Hardcastle AJ, Vincent AL. Further genetic and clinical insights of posterior polymorphous corneal dystrophy 3. JAMA Ophthalmol 2013; 131:1296-303. [PMID: 23807282].

16. Evans CJ, Liskova P, Dudakova L, Hrabcikova P, Horinek A, Jirsova K, Filipec M, Hardcastle AJ, Davidson AE, Tuft SJ. Identification of six novel mutations in ZEB1 and description of the associated phenotypes in patients with posterior polymorphous corneal dystrophy 3. Ann Hum Genet 2015; 79:1-9. [PMID: 25441224].

17. Liskova P, Evans CJ, Davidson AE, Zaliova M, Dudakova L, Trkova M, Stranecky V, Carnt N, Plagnol V, Vincent AL, Tuft SJ, Hardcastle AJ. Heterozygous deletions at the ZEB1 locus verify haploinsufficiency as the mechanism of disease for posterior polymorphous corneal dystrophy type 3. Eur J Hum Genet 2016; 24:985-91. [PMID: 26508574].

18. Lee B, Villarreal-Ponce A, Fallahi M, Ovadia J, Sun P, Yu QC, Ito S, Sinha S, Nie Q, Dai X. Transcriptional mechanisms link epithelial plasticity to adhesion and differentiation of epidermal progenitor cells. Dev Cell 2014; 29:47-58. [PMID: 24735878].

19. Watanabe K, Villarreal-Ponce A, Sun P, Salmans ML, Fallahi M, Andersen B, Dai X. Mammary morphogenesis and regeneration require the inhibition of EMT at terminal end buds by Ovol2 transcriptional repressor. Dev Cell 2014; 29:59-74. [PMID: 24735879].

20. Kitazawa K, Hikichi T, Nakamura T, Mitsunaga K, Tanaka A, Nakamura M, Yamakawa T, Furukawa S, Takasaka M, Goshima N, Watanabe A, Okita K, Kawasaki S, Ueno M, Kinoshita S, Masui S. OVOL2 Maintains the Transcriptional Program of Human Corneal Epithelium by Suppressing Epithelial-to-Mesenchymal Transition. Cell Reports 2016; 15:1359-68. [PMID: 27134177].

21. Hong T, Watanabe K, Ta CH, Villarreal-Ponce A, Nie Q, Dai X. An Ovol2-Zeb1 Mutual Inhibitory Circuit Governs Bidirectional and Multi-step Transition between Epithelial and Mesenchymal States. PLOS Comput Biol 2015; 11:e1004569-[PMID: 26554584].

22. Lamouille S, Xu J, Derynck R. Molecular mechanisms of epithelial-mesenchymal transition. Nat Rev Mol Cell Biol 2014; 15:178-96. [PMID: 24556840].

23. Roca H, Hernandez J, Weidner S, McEachin RC, Fuller D, Sud S, Schumann T, Wilkinson JE, Zaslavsky A, Li H, Maher CA, Daignault-Newton S, Healy PN, Pienta KJ. Transcription factors OVOL1 and OVOL2 induce the mesenchymal to epithelial transition in human cancer. PLoS One 2013; 8:e76773-[PMID: 24124593].

24. Chung DD, Frausto RF, Lin BR, Hanser EM, Cohen Z, Aldave AJ. Transcriptomic Profiling of Posterior Polymorphous Corneal Dystrophy. Invest Ophthalmol Vis Sci 2017; 58:3202-14. [PMID: 28654985].

25. Merjava S, Malinova E, Liskova P, Filipec M, Zemanova Z, Michalova K, Jirsova K. Recurrence of posterior polymorphous corneal dystrophy is caused by the overgrowth of the

original diseased host endothelium. Histochem Cell Biol 2011; 136:93-101. [PMID: 21695473].

26. Jirsova K, Merjava S, Martincova R, Gwilliam R, Ebenezer ND, Liskova P, Filipec M. Immunohistochemical characterization of cytokeratins in the abnormal corneal endothelium of posterior polymorphous corneal dystrophy patients. Exp Eye Res 2007; 84:680-6. [PMID: 17289024].

27. Schmedt T, Chen Y, Nguyen TT, Li S, Bonanno JA, Jurkunas UV. Telomerase immortalization of human corneal endothelial cells yields functional hexagonal monolayers. PLoS One 2012; 7:e51427-[PMID: 23284695].

28. Frausto RF, Le DJ, Aldave AJ. Transcriptomic Analysis of Cultured Corneal Endothelial Cells as a Validation for Their Use in Cell Replacement Therapy. Cell Transplant 2016; 25:1159-76. [PMID: 26337789].

29. Schneider CA, Rasband WS, Eliceiri KW. NIH Image to ImageJ: 25 years of image analysis. Nat Methods 2012; 9:671-5. [PMID: 22930834].

30. Pop C, Salvesen GS. Human caspases: activation, specificity, and regulation. J Biol Chem 2009; 284:21777-81. [PMID: 19473994].

31. Stolwijk JA, Matrougui K, Renken CW, Trebak M. Impedance analysis of GPCR-mediated changes in endothelial barrier function: overview and fundamental considerations for stable and reproducible measurements. Pflugers Arch 2015; 467:2193-218. [PMID: 25537398].

32. Koeppe L. Klinische Beobachtunigen mit der Nernstspaltlampe und dem Hornhautmikroskop. Albrecht Von Graefes Arch Ophthalmol 1916; 91:375-9. .

33. Gasset AR, Zimmerman TJ. Posterior polymorphous dystrophy associated with keratoconus. Am J Ophthalmol 1974; 78:535-7. [PMID: 4547273].

34. Lam HY, Wiggs JL, Jurkunas UV. Unusual presentation of presumed posterior polymorphous dystrophy associated with iris heterochromia, band keratopathy, and keratoconus. Cornea 2010; 29:1180-5. [PMID: 20567203].

35. Aldave AJ, Ann LB, Frausto RF, Nguyen CK, Yu F, Raber IM. Classification of posterior polymorphous corneal dystrophy as a corneal ectatic disorder following confirmation of associated significant corneal steepening. JAMA Ophthalmol 2013; 131:1583-90. [PMID: 24113819].

36. Grayson M. The nature of hereditary deep polymorphous dystrophy of the cornea: its association with iris and anterior chamber dygenesis. Trans Am Ophthalmol Soc 1974; 72:516-59. [PMID: 4549335].

37. Henriquez AS, Kenyon KR, Dohlman CH, Boruchoff SA, Forstot SL, Meyer RF, Hanninen LA. Morphologic characteristics of posterior polymorphous dystrophy. A study of nine corneas and review of the literature. Surv Ophthalmol 1984; 29:139-47. [PMID: 6334374].

38. Boruchoff SA, Kuwabara T. Electron microscopy of posterior polymorphous degeneration. Am J Ophthalmol 1971; 72:879-87. [PMID: 4940980].

39. Rodrigues MM, Sun TT, Krachmer J, Newsome D. Epithelialization of the corneal endothelium in posterior polymorphous dystrophy. Invest Ophthalmol Vis Sci 1980; 19:832-5. [PMID: 6156141].

40. Rodrigues MM, Newsome DA, Krachmer JH, Sun TT. Posterior polymorphous dystrophy of the cornea: cell culture studies. Exp Eye Res 1981; 33:535-44. [PMID: 7032957].

41. Bozkurt B, Irkec M, Mocan MC. In vivo confocal microscopic findings in posterior polymorphous corneal dystrophy. Cornea 2013; 32:1237-42. [PMID: 23635854].

42. Shiraishi A, Zheng X, Sakane Y, Hara Y, Hayashi Y. In vivo confocal microscopic observations of eyes diagnosed with posterior corneal vesicles. Jpn J Ophthalmol 2016; 60:425-32. [PMID: 27585920].

43. Kalluri R, Weinberg RA. The basics of epithelial-mesenchymal transition. J Clin Invest 2009; 119:1420-8. [PMID: 19487818].

44. Chen T, You Y, Jiang H, Wang ZZ. Epithelial-Mesenchymal Transition (EMT): A Biological Process in the Development, Stem Cell Differentiation and Tumorigenesis. J Cell Physiol 2017; [PMID: 28079253].

45. Pradella D, Naro C, Sette C, Ghigna C. EMT and stemness: flexible processes tuned by alternative splicing in development and cancer progression. Mol Cancer 2017; 16:8-[PMID: 28137272].

46. Maeda M, Johnson KR, Wheelock MJ. Cadherin switching: essential for behavioral but not morphological changes during an epithelium-to-mesenchyme transition. J Cell Sci 2005; 118:873-87. [PMID: 15713751].

47. Wheelock MJ, Shintani Y, Maeda M, Fukumoto Y, Johnson KR. Cadherin switching. J Cell Sci 2008; 121:727-35. [PMID: 18322269].

48. Sanchez-Tillo E, Fanlo L, Siles L, Montes-Moreno S, Moros A, Chiva-Blanch G, Estruch R, Martinez A, Colomer D, Gyorffy B, Roue G, Postigo A. The EMT activator ZEB1 promotes tumor growth and determines differential response to chemotherapy in mantle cell lymphoma. Cell Death Differ 2014; 21:247-57. [PMID: 24013721].

49. Zhang P, Sun Y, Ma L. ZEB1: at the crossroads of epithelial-mesenchymal transition, metastasis and therapy resistance. Cell Cycle 2015; 14:481-7. [PMID: 25607528].

50. Liu Y, Peng X, Tan J, Darling DS, Kaplan HJ, Dean DC. Zeb1 mutant mice as a model of posterior corneal dystrophy. Invest Ophthalmol Vis Sci 2008; 49:1843-9. [PMID: 18436818].

51. Zhu YT, Chen HC, Chen SY, Tseng SC. Nuclear p120 catenin unlocks mitotic block of contact-inhibited human corneal endothelial monolayers without disrupting adherent junctions. J Cell Sci 2012; 125:3636-48. [PMID: 22505615].

52. Roy O, Leclerc VB, Bourget JM, Theriault M, Proulx S. Understanding the process of corneal endothelial morphological change in vitro. Invest Ophthalmol Vis Sci 2015; 56:1228-37. [PMID: 25698769].

53. Gal A, Sjoblom T, Fedorova L, Imreh S, Beug H, Moustakas A. Sustained TGF beta exposure suppresses Smad and

non-Smad signalling in mammary epithelial cells, leading to EMT and inhibition of growth arrest and apoptosis. Oncogene 2008; 27:1218-30. [PMID: 17724470].

54. Gu Y, Zhao Y, Zhou Y, Xie Y, Ju P, Long Y, Liu J, Ni D, Cao F, Lyu Z, Mao Z, Hao J, Li Y, Wan Q, Kanyomse Q, Liu Y, Ren D, Ning Y, Li X, Zhou Q, Li B. Zeb1 Is a Potential Regulator of Six2 in the Proliferation, Apoptosis and Migration of Metanephric Mesenchyme Cells. Int J Mol Sci 2016; 17:pii: E1283-[PMID: 27509493].

55. Postigo AA. Opposing functions of ZEB proteins in the regulation of the TGFbeta/BMP signaling pathway. EMBO J 2003; 22:2443-52. [PMID: 12743038].

56. Postigo AA, Dean DC. ZEB represses transcription through interaction with the corepressor CtBP. Proc Natl Acad Sci USA 1999; 96:6683-8. [PMID: 10359772].

57. Postigo AA, Depp JL, Taylor JJ, Kroll KL. Regulation of Smad signaling through a differential recruitment of coactivators and corepressors by ZEB proteins. EMBO J 2003; 22:2453-62. [PMID: 12743039].

58. Nicholson DW, Ali A, Thornberry NA, Vaillancourt JP, Ding CK, Gallant M, Gareau Y, Griffin PR, Labelle M, Lazebnik YA, Munday . NARaju . SMSmulson . MEYamin . TYu . VLMiller . DKIdentification and inhibition of the ICE/CED-3 protease necessary for mammalian apoptosis. Nature 1995; 376:37-43. [PMID: 7596430].

59. Ahn YJ, Choi SI, Yum HR, Shin SY, Park SH. Clinical Features in Children with Posterior Polymorphous Corneal Dystrophy. Optom Vis Sci 2016; [PMID: 28009792].

60. Bonanno JA. Identity and regulation of ion transport mechanisms in the corneal endothelium. Prog Retin Eye Res 2003; 22:69-94. [PMID: 12597924].

61. Harris JE. Current thoughts on the maintenance of corneal hydration in vivo. Arch Ophthalmol 1967; 78:126-32. [PMID: 4952923].

62. Noske W, Fromm M, Levarlet B, Kreusel KM, Hirsch M. Tight junctions of the human corneal endothelium: morphological and electrophysiological features. Ger J Ophthalmol 1994; 3:253-7. [PMID: 7804113].

63. Yokoi N, Yoshizaki K, Kinoshita S, Morimoto T. Proton nuclear magnetic resonance study on the barrier function of pig corneal epithelium and endothelium. Jpn J Ophthalmol 1995; 39:216-24. [PMID: 8577071].

64. Levy SG, Moss J, Noble BA, McCartney AC. Early-onset posterior polymorphous dystrophy. Arch Ophthalmol 1996; 114:1265-8. [PMID: 8859091].

65. Moroi SE, Gokhale PA, Schteingart MT, Sugar A, Downs CA, Shimizu S, Krafchak C, Fuse N, Elner SG, Elner VM, Flint A, Epstein MP, Boehnke M, Richards JE. Clinicopathologic correlation and genetic analysis in a case of posterior polymorphous corneal dystrophy. Am J Ophthalmol 2003; 135:461-70. [PMID: 12654361].

66. Bonanno JA. Molecular mechanisms underlying the corneal endothelial pump. Exp Eye Res 2012; 95:2-7. [PMID: 21693119].

67. Fischbarg J. Fluid transport across leaky epithelia: central role of the tight junction and supporting role of aquaporins. Physiol Rev 2010; 90:1271-90. [PMID: 20959616].

Articles are provided courtesy of Emory University and the Zhongshan Ophthalmic Center, Sun Yat-sen University, P.R. China. The print version of this article was created on 14 October 2017. This reflects all typographical corrections and errata to the article through that date. Details of any changes may be found in the online version of the article.